



The semi-constrained NMSSM satisfying bounds from the LHC, LUX and Planck

Ulrich Ellwanger, Cyril Hugonie

► To cite this version:

Ulrich Ellwanger, Cyril Hugonie. The semi-constrained NMSSM satisfying bounds from the LHC, LUX and Planck. *Journal of High Energy Physics*, 2014, 1408, pp.046. 10.1007/JHEP08(2014)046 . hal-00996033

HAL Id: hal-00996033

<https://hal.science/hal-00996033>

Submitted on 26 May 2014

HAL is a multi-disciplinary open access archive for the deposit and dissemination of scientific research documents, whether they are published or not. The documents may come from teaching and research institutions in France or abroad, or from public or private research centers.

L'archive ouverte pluridisciplinaire **HAL**, est destinée au dépôt et à la diffusion de documents scientifiques de niveau recherche, publiés ou non, émanant des établissements d'enseignement et de recherche français ou étrangers, des laboratoires publics ou privés.

The semi-constrained NMSSM satisfying bounds from the LHC, LUX and Planck

Ulrich Ellwanger^a and Cyril Hugonie^b

^a *LPT, UMR 8627, CNRS, Université de Paris–Sud, 91405 Orsay, France*

^b *LUPM, UMR 5299, CNRS, Université de Montpellier II, 34095 Montpellier, France*

Abstract

We study the parameter space of the semi-constrained NMSSM, compatible with constraints on the Standard Model like Higgs mass and signal rates, constraints from searches for squarks and gluinos, a dark matter relic density compatible with bounds from WMAP/Planck, and direct detection cross sections compatible with constraints from LUX. The remaining parameter space allows for a fine-tuning as low as about 100, an additional lighter Higgs boson in the 60-120 GeV mass range detectable in the diphoton mode or in decays into a pair of lighter CP-odd Higgs bosons, and dominantly singlino like dark matter with a mass down to 1 GeV, but possibly a very small direct detection cross section.

1 Introduction

Recent results from the LHC and direct dark matter detection experiments constrain considerably possible scenarios beyond the Standard Model (SM), amongst others its supersymmetric (SUSY) extensions. These constraints originate essentially from the Higgs mass [1, 2] and its quite SM like signal rates, the absence of signals in searches for squarks and gluinos after the 8 TeV run at the LHC [3, 4], and upper bounds on dark matter–nucleus cross sections from the LUX experiment [5].

Masses and couplings of Higgs boson(s), SUSY particles and notably the lightest SUSY particle (LSP, the dark matter candidate), are strongly correlated in SUSY extensions of the SM if one assumes at least partial unification of the soft SUSY breaking terms at a grand unification (GUT) scale. Hence it is interesting to study how the combined constraints affect the parameter space and, notably, which signals beyond the SM we can expect in the future. Such studies (after the discovery of the 126 GeV Higgs boson) had been performed earlier in the Minimal SUSY extension of the SM (MSSM) [6–26] and the Next-to-Minimal SUSY extension of the SM (NMSSM) [7, 24, 27–31].

These studies differ, however, in the treatment of the soft SUSY breaking terms in the Higgs sector at the GUT scale: In “fully constrained” versions of the MSSM or NMSSM these are supposed to be unified with the soft SUSY breaking terms in the squark and slepton sectors. In NUHM (non-universal Higgs masses) or “semi-constrained” versions of the MSSM or NMSSM one allows the soft SUSY breaking terms in the Higgs sector to be different; after all the quantum numbers of the Higgs fields differ from those of quarks and leptons: Higgs fields are in a real representation $(2 + 2)$ of $SU(2)$, but do not fit into complete representations of $SU(5)$; these properties can easily have an impact on the presently unknown sources of soft SUSY breaking terms. In the NMSSM including the singlet superfield S , “semi-constrained” can indicate non-universal soft SUSY breaking terms involving the singlet only, or non-universal soft SUSY breaking terms involving $SU(2)$ doublet or singlet Higgs fields. In the present study we allow for the latter more general case.

Previous studies of the NMSSM with constraints at the GUT scale [24, 27–31] had found that wide ranges of parameter space comply with constraints from the LHC and on dark matter, and that less “tuning” is required than in the MSSM [24, 30]. These findings are confirmed by scans of the parameter space of the general NMSSM (without constraints at the GUT scale) [32–38], and motivate a thorough analysis of the semi-constrained NUH-NMSSM with up-to-date experimental constraints, amongst others on Higgs signal rates and bounds on dark matter–nucleus cross sections [5]. “NUH” appears without “M” since, apart from the Higgs mass terms, also trilinear couplings involving Higgs bosons only are allowed to differ from trilinear couplings involving squarks or sleptons at the GUT scale, see the next section.

Using the code `NMSPEC` [40] within `NMSSMTools_4.2.1` [41, 42] together with `micrOMEGAS_3` [43] we have sampled about 3.2 M viable points in the parameter space, which allows us to cover the complete range of masses and couplings of the LSP and additional Higgs bosons, parts of which had not been observed in previous analyses. In this paper we confine ourselves to regions where an additional NMSSM-specific Higgs scalar is lighter than the SM-like Higgs boson near 126 GeV; this region is strongly favoured by the mass of the SM-like Higgs boson, and contains the most interesting phenomena to be searched for in the future.

In the next section we present the model, the applied phenomenological constraints, the

definition of fine-tuning, and the ranges of parameters scanned over. In section 3 we discuss the impact of unsuccessful searches for squarks and gluinos at the LHC on fine-tuning and some of the parameters like the soft squark/slepton masses m_0 , the universal gaugino masses $M_{1/2}$ and the NMSSM-specific Yukawa coupling λ . Section 4 is devoted to the properties of the LSP, its detection rates to be expected in the future, and its annihilation processes allowing for a viable relic density. In section 5 we discuss the Higgs sector, in particular prospects to detect the lighter NMSSM specific Higgs scalar. Conclusions and an outlook are given in section 6.

2 The NMSSM with constraints at the GUT scale

The NMSSM [44] differs from the MSSM due to the presence of the gauge singlet superfield S . In the simplest \mathbb{Z}_3 invariant realisation of the NMSSM, the Higgs mass term $\mu H_u H_d$ in the superpotential W_{MSSM} of the MSSM is replaced by the coupling λ of S to H_u and H_d and a self-coupling κS^3 . Hence, in this simplest version the superpotential W_{NMSSM} is scale invariant and given by

$$W_{\text{NMSSM}} = \lambda \hat{S} \hat{H}_u \cdot \hat{H}_d + \frac{\kappa}{3} \hat{S}^3 + \dots, \quad (2.1)$$

where hatted letters denote superfields, and the ellipses denote the MSSM-like Yukawa couplings of \hat{H}_u and \hat{H}_d to the quark and lepton superfields. Once the real scalar component of \hat{S} develops a vev s , the first term in W_{NMSSM} generates an effective μ -term

$$\mu_{\text{eff}} = \lambda s. \quad (2.2)$$

The soft Susy breaking terms consist of mass terms for the Higgs bosons H_u , H_d , S , squarks $\tilde{q}_i \equiv (\tilde{u}_{iL}, \tilde{d}_{iL})$, \tilde{u}_{iR}^c , \tilde{d}_{iR}^c and sleptons $\tilde{\ell}_i \equiv (\tilde{\nu}_{iL}, \tilde{e}_{iL})$ and \tilde{e}_{iR}^c (where $i = 1, 2, 3$ is a generation index):

$$\begin{aligned} -\mathcal{L}_0 = & m_{H_u}^2 |H_u|^2 + m_{H_d}^2 |H_d|^2 + m_S^2 |S|^2 + m_{\tilde{q}_i}^2 |\tilde{q}_i|^2 + m_{\tilde{u}_i}^2 |\tilde{u}_{iR}^c|^2 + m_{\tilde{d}_i}^2 |\tilde{d}_{iR}^c|^2 \\ & + m_{\tilde{\ell}_i}^2 |\tilde{\ell}_i|^2 + m_{\tilde{e}_i}^2 |\tilde{e}_{iR}^c|^2, \end{aligned} \quad (2.3)$$

trilinear interactions involving the third generation squarks, sleptons and the Higgs fields (neglecting the Yukawa couplings of the two first generations):

$$\begin{aligned} -\mathcal{L}_3 = & \left(h_t A_t Q \cdot H_u \tilde{u}_{3R}^c + h_b A_b H_d \cdot Q \tilde{d}_{3R}^c + h_\tau A_\tau H_d \cdot L \tilde{e}_{3R}^c \right. \\ & \left. + \lambda A_\lambda H_u \cdot H_d S + \frac{1}{3} \kappa A_\kappa S^3 \right) + \text{h.c.}, \end{aligned} \quad (2.4)$$

and mass terms for the gauginos \tilde{B} (bino), \tilde{W}^a (winos) and \tilde{G}^a (gluinos):

$$-\mathcal{L}_{1/2} = \frac{1}{2} \left[M_1 \tilde{B} \tilde{B} + M_2 \sum_{a=1}^3 \tilde{W}^a \tilde{W}_a + M_3 \sum_{a=1}^8 \tilde{G}^a \tilde{G}_a \right] + \text{h.c.} \quad (2.5)$$

In constrained versions of the NMSSM one assumes that the soft Susy breaking terms involving gauginos, squarks or sleptons are identical at the GUT scale:

$$M_1 = M_2 = M_3 \equiv M_{1/2}, \quad (2.6)$$

$$m_{\tilde{q}_i}^2 = m_{\tilde{u}_i}^2 = m_{\tilde{d}_i}^2 = m_{\tilde{t}_i}^2 = m_{\tilde{e}_i}^2 \equiv m_0^2, \quad (2.7)$$

$$A_t = A_b = A_\tau \equiv A_0. \quad (2.8)$$

In the NUH-NMSSM considered here one allows the Higgs sector to play a special role: The Higgs soft mass terms $m_{H_u}^2$, $m_{H_d}^2$ and m_S^2 are allowed to differ from m_0^2 (and determined implicitly at the weak scale by the three minimization equations of the effective potential), and the trilinear couplings A_λ , A_κ can differ from A_0 . Hence the complete parameter space is characterized by

$$\lambda, \kappa, \tan\beta, \mu_{\text{eff}}, A_\lambda, A_\kappa, A_0, M_{1/2}, m_0, \quad (2.9)$$

where the latter five parameters are taken at the GUT scale.

Expressions for the mass matrices of the physical CP-even and CP-odd Higgs states – after H_u , H_d and S have assumed vevs v_u , v_d and s and including the dominant radiative corrections – can be found in [44] and will not be repeated here. The physical CP-even Higgs states will be denoted as H_i , $i = 1, 2, 3$ (ordered in mass), and the physical CP-odd Higgs states as A_i , $i = 1, 2$. The neutralinos are denoted as χ_i^0 , $i = 1, \dots, 5$ and their mixing angles $N_{i,j}$ such that $N_{1,5}$ indicates the singlino component of the lightest neutralino χ_1^0 .

Subsequently we are interested in regions of the parameter space where doublet-singlet mixing in the Higgs sector leads to an increase of the mass of the SM-like (mostly doublet-like) Higgs boson, which leads naturally to a SM-like Higgs boson H_2 in the 126 GeV range [32, 33, 45–48], but implies a lighter mostly singlet-like Higgs state H_1 .

Recent phenomenological constraints include, amongst others, upper bounds on the direct (spin independent) detection rate of dark matter by LUX [5]. In the NMSSM, the LSP (the dark matter candidate) is assumed to be the lightest neutralino, as in the MSSM. Its spin independent detection rate and relic density are computed with the help of `micrOMEGAS` 3 [43]. We apply the upper bounds of LUX and require a relic density inside a slightly enlarged WMAP/Planck window [49, 50] $0.107 \leq \Omega h^2 \leq 0.131$ in order not to lose too many points in parameter space; the precise value of Ωh^2 has little impact on the subsequent results.

In the Higgs sector we require a neutral CP-even state with a mass of 125.7 ± 3 GeV allowing for theoretical and parametric uncertainties of the mass calculation; we used 173.1 GeV for the top quark mass. Its signal rates should comply with the essentially SM-like signal rates in the channels measured by ATLAS/CMS/Tevatron. These measurements can be combined leading to 95% confidence level (CL) contours in the planes of Higgs production via (gluon fusion and $t\bar{t}H$) – (vector boson fusion and associate production with W/Z), separately for Higgs decays into $\gamma\gamma$, ZZ or WW and $b\bar{b}$ or $\tau^+\tau^-$. We require that the signal rates for a Higgs boson in the above mass range are within all three 95% confidence level contours derived in [51].

The application of constraints from unsuccessful searches for sparticles at the first run of the LHC is more delicate: These bounds depend on all parameters of the model via the masses and couplings (and the resulting decay cascades) of all sparticles. However, it is possible to proceed as follows, using the most constraining searches for gluinos and squarks of the first generation in events with jets and missing E_T : For heavy squarks and/or gluinos the production cross sections are so small that these points in parameter space are not excluded independently of the squark/gluino decay cascades. On the other hand, relatively light squarks and/or gluinos are excluded independently of their decay cascades. In between these regions defined in the planes of squark/gluino masses or $m_0/M_{1/2}$, exclusion does depend on their decays, in particular on the presence of a light singlino-like LSP at the end of the cascades [52, 53].

The boundaries between these three regions were obtained with the help of the analysis of some hundreds of points in parameter space: Events were generated by MadGraph/MadEvent [54] which includes Pythia 6.4 [55] for showering and hadronisation. The sparticle branching ratios are obtained with the help of the code NMSDECAY [56] (based on SDECAY [57]), and are passed to Pythia. The output in StdHEP format is given to CheckMATE [58] which includes the detector simulation DELPHES [59] and compares the signal rates to constraints in various search channels of ATLAS and CMS. Corresponding results will be presented in section 3.

Other constraints from b -physics, LEP (from Higgs searches and invisible Z decays) and the LHC (on heavy Higgs bosons decaying into $\tau^+\tau^-$) are applied as in **NMSSMTools_4.2.1** [41, 42], leaving aside the muon anomalous magnetic moment.

Since the fundamental parameters of the model are the masses and couplings at the GUT scale, it makes sense to ask in how far these have to be tuned relative to each other in order to comply with the SM-like Higgs mass and the non-observation of sparticles at the LHC. To this end we consider the usual measure of fine-tuning [60]

$$FT = \text{Max} \left\{ \left| \frac{\partial \ln(M_Z)}{\partial \ln(p_i^{GUT})} \right| \right\} \quad (2.10)$$

where p_i^{GUT} denote all dimensionful and dimensionless parameters (Yukawa couplings, mass terms and trilinear couplings) at the GUT scale. FT is computed numerically in **NMSSMTools_4.2.1** following the method described in [61] where details can be found.

We have scanned the parameter space of the NUH-NMSSM given in (2.9) using a Markov Chain Monte Carlo (MCMC) technique. In addition to the phenomenological constraints discussed above we require the absence of Landau singularities of the running Yukawa couplings below the GUT scale, and the absence of deeper unphysical minima of the Higgs potential with at least one vanishing vev v_u , v_d or s . Bounds on the dimensionful parameters follow from the absence of too large fine-tuning; we imposed $FT < 1000$. Finally we obtained $\sim 3.2 \times 10^6$ valid points in parameter space within the following ranges of the parameters (2.9):

$$\begin{aligned} 1 \times 10^{-6} \leq \lambda \leq 0.722, \quad & -0.08 \leq \kappa \leq 0.475, \quad & 1.42 \leq \tan \beta \leq 60.3, \\ -537 \text{ GeV} \leq \mu_{\text{eff}} \leq 753 \text{ GeV}, \quad & -19 \text{ TeV} \leq A_\lambda \leq 8.5 \text{ TeV}, \quad & -1.3 \text{ TeV} \leq A_\kappa \leq 5.3 \text{ TeV}, \\ 0 \text{ GeV} \leq m_0 \leq 4.4 \text{ TeV}, \quad & 0.1 \text{ TeV} \leq M_{1/2} \leq 3.1 \text{ TeV}, \quad & -6.6 \text{ TeV} \leq A_0 \leq 8.1 \text{ TeV}. \end{aligned} \quad (2.11)$$

The fact that the upper bounds on the dimensionful parameters are distinct originates from the different impact of these parameters on the fine-tuning, which is often dominated by the universal gaugino mass parameter $M_{1/2}$.

3 Impact of LHC constraints on squark/gluino masses and fine-tuning

Strong constraints on parameter spaces of SUSY extensions of the SM come from searches for gluinos \tilde{g} and squarks \tilde{q} of the first generation in events with jets and missing E_T [3, 4].

In [3] exclusion limits for MSUGRA/CMSSM models have been given in the $m_0 - M_{1/2}$ and $M_{\tilde{g}} - m_{\tilde{q}}$ planes for $\tan\beta = 30$, $A_0 = -2m_0$ and $\mu > 0$.

As a result of the simulations described in the previous section we found that the 95% CL upper limits on signal events in [3] lead to exclusion limits in the $m_0 - M_{1/2}$ or $M_{\tilde{g}} - m_{\tilde{q}}$ planes in the NUH-NMSSM which are very similar to the CMSSM if the LSP is bino-like, but can be alleviated in the presence of a light singlino-like LSP at the end of the cascades [52, 53]. Still, even with a singlino-like LSP, certain regions in these planes are always excluded.

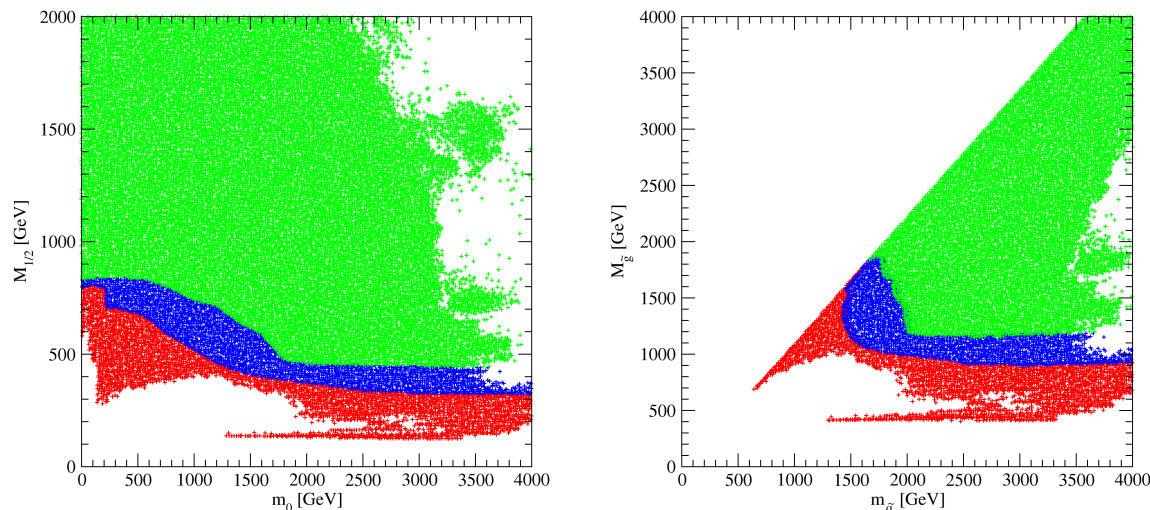


Figure 1: The $m_0 - M_{1/2}$ and $M_{\tilde{g}} - m_{\tilde{q}}$ planes in the NUH-NMSSM. Green: regions allowed by the 95% CL upper limits on signal events in [3], blue: regions allowed in the presence of a singlino-like LSP, red: regions which are always excluded.

In Fig. 1 we show the $m_0 - M_{1/2}$ and $M_{\tilde{g}} - m_{\tilde{q}}$ planes in the NUH-NMSSM and indicate in green the regions allowed by the 95% CL upper limits on signal events (practically identical to the ones given in [3]), in blue the regions possibly allowed in the presence of a singlino-like LSP, and in red the regions which are always excluded. Note that, in contrast to the MSSM, the limit $m_0 \rightarrow 0$ is always possible for all $M_{1/2}$: In the MSSM this region is limited by the appearance of a stau LSP. In the NMSSM a singlino-like LSP can always be lighter than the lightest stau, and its relic density can be reduced to the WMAP/Planck window through singlino-stau coannihilation as in the fully constrained NMSSM [62, 63] or through narrow resonances implying specific NMSSM light Higgs states [34, 67–69]. (The combined constraints from the Higgs sector and the nature of the LSP lead to discontinuities in the allowed parameter space for small m_0 .)

These lower bounds on the squark and gluino masses dominate the lower bounds on the fine-tuning FT defined in (2.10). In Fig. 2 we show FT as function of the squark and gluino masses, and the impact of the LHC constraints in the same color coding as in Fig. 1.

We see that the LHC forbidden red region increases the lower bound on FT from ~ 20 to $FT \gtrsim 80$; the NMSSM-specific alleviation (blue region) has a minor impact on FT . The dominant contribution to FT in (2.10) originates typically from $M_{1/2}$ (i.e. the gluino mass at

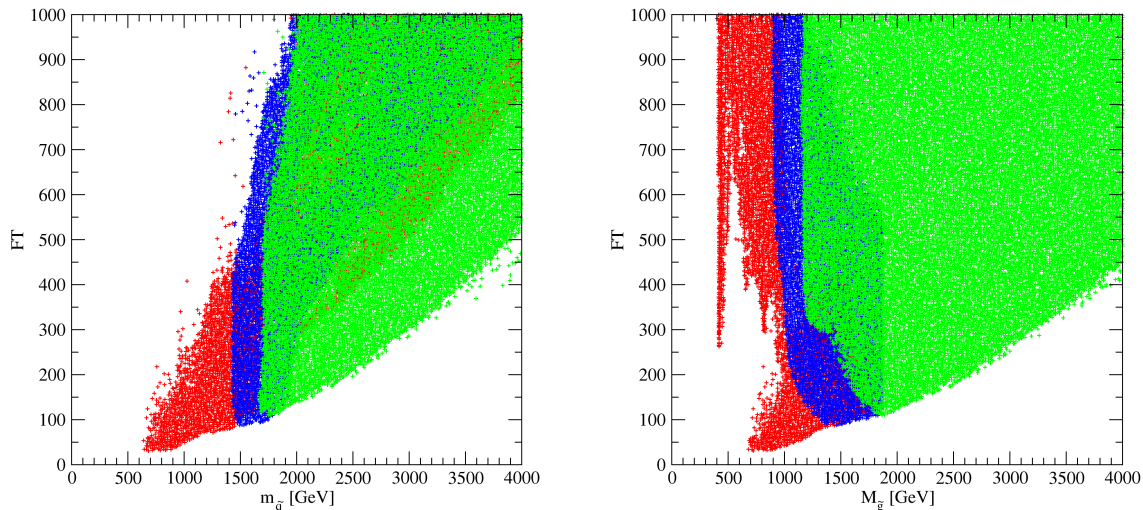


Figure 2: FT as defined in (2.10) as function of the squark and gluino masses, and the impact of the LHC constraints in the same color coding as in Fig. 1.

the GUT scale), or from the soft Higgs mass term $m_{H_u}^2$. If one requires unification of m_{H_u} and m_{H_d} with m_0 as in [30], FT is considerably larger ($\gtrsim 400$). In the MSSM – after imposing LHC constraints on squark and gluino masses, defining FT with respect to parameters at the GUT scale and allowing for non-universal Higgs mass terms at the GUT scale as in [64] – one finds $FT \gtrsim 1000$. The much lower value of FT in the NUH-NMSSM coincides with the result in [65].

The impact of $M_{1/2}$ on FT is actually indirect: Heavy gluinos lead to large radiative corrections to the stop masses which, in turn, lead to large radiative corrections to the soft Higgs mass terms. Therefore, if one defines FT with respect to parameters at a lower scale, low FT is typically related to light stops. On the left-hand side of Fig. 3 we show FT as function of the mass $m_{\tilde{t}_1}$ of the lightest stop. We see that, without imposing LHC constraints on squark and gluino masses, the lower bound on FT (still with respect to parameters at the GUT scale) would increase slightly with $m_{\tilde{t}_1}$, but with LHC constraints the lower bound on FT depends weakly on (decreases only slightly with) $m_{\tilde{t}_1}$.

In the MSSM, the measured mass of the SM-like Higgs H_{SM} requires relatively heavy stops and/or a Higgs-stop trilinear coupling A_t , which also contribute to FT . In the NMSSM (recall that, in the scenario considered here, $H_{SM} = H_2$) large radiative corrections to the SM-like Higgs mass $m_{H_{SM}}$ are not required, since the SM-like Higgs mass can be pushed upwards either through a positive tree level contribution $\sim \lambda^2 \sin^2 2\beta$ [44], or through mixing with a lighter Higgs state H_1 [66] which does not require large values of λ [71]. (In the latter scenario too large values of λ , i.e. a too large $H_1 - H_{SM}$ mixing angle, can imply an unacceptable reduction of the signal rates of H_{SM} at the LHC and/or lead to the violation of LEP constraints on H_1 .)

On the right-hand side of Fig. 3 we show FT as function of λ . We see that – without imposing LHC constraints on squark and gluino masses – the minimum of FT would indeed be assumed for $\lambda \sim 0.6$ related to the tree level contribution $\sim \lambda^2 \sin^2 2\beta$ to $m_{H_{SM}}$. Including

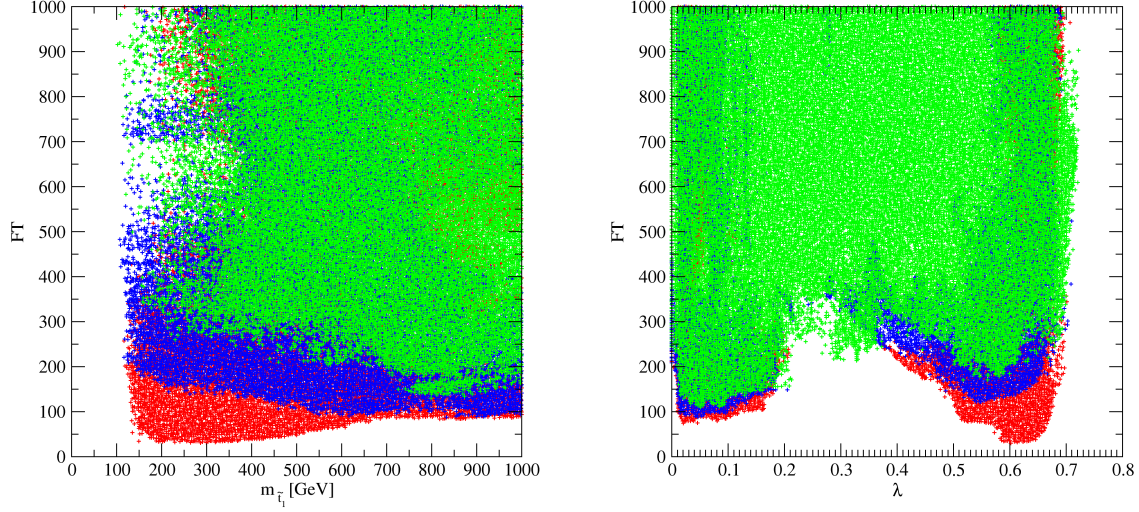


Figure 3: Left: FT as function of the $m_{\tilde{t}_1}$. Right: FT as function of λ at the SUSY scale. The color coding is as in Fig. 1.

LHC constraints, local minima of FT exist both for $\lambda \approx 0.6$ and $\lambda \approx 0.1$.

Since the increase of the SM-like Higgs mass with the help of the tree level contribution $\sim \lambda^2 \sin^2 2\beta$ is effective only for large λ but relatively low $\tan\beta$, these regions are typically correlated which is clarified on the left hand side of Fig. 4. On the right hand side we show the correlations between λ and κ which shows that larger κ are typically related to larger λ .

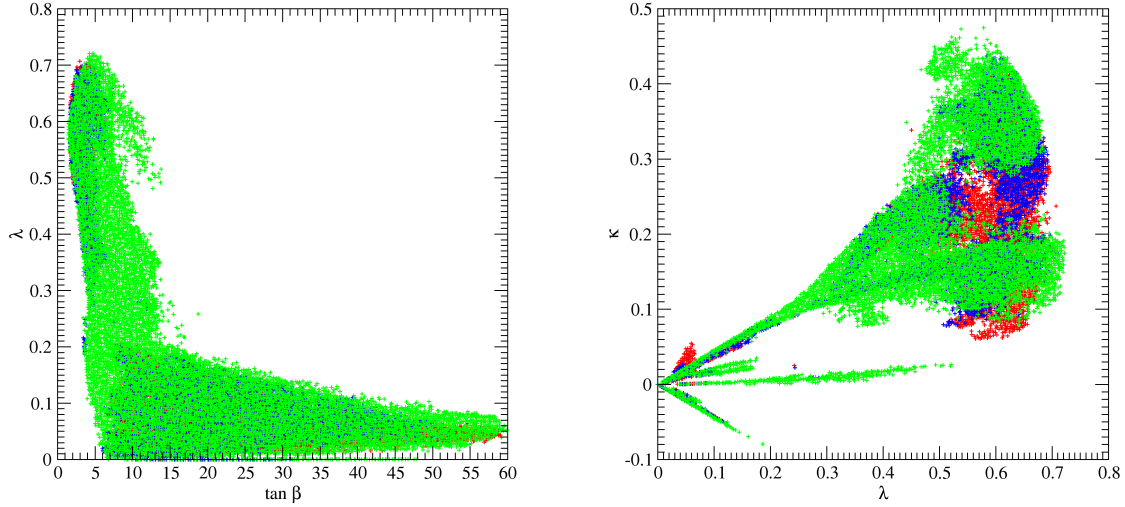


Figure 4: Left: λ as function of $\tan\beta$. Right: κ as function of λ . The colors are as in Fig. 1.

Herewith we conclude the discussion of the impact of LHC constraints on FT and the corresponding correlations with other parameters.

4 Properties of dark matter

Besides the enlarged Higgs sector, the enlarged neutralino sector of the NMSSM can have a significant phenomenological impact. The LSP (the lightest neutralino χ_1^0) can have a dominant singlino component and still be an acceptable candidate for dark matter. Its relic density can be reduced to fit in the WMAP/Planck window, amongst others, via the exchange of NMSSM-specific CP-even or CP-odd Higgs scalars in the s-channel [34, 67–69], whereas its direct detection cross section can be very small.

The latter feature is clarified in Fig. 5 where we show the spin-independent χ_1^0 -nucleon cross section (after imposing constraints from the LUX experiment [5]) as function of $M_{\chi_1^0}$. We focus on χ_1^0 masses below 100 GeV since no additional interesting features appear for larger $M_{\chi_1^0}$, but the region of small $M_{\chi_1^0}$ exhibits structures which ask for explanations.

In Fig. 5 we have indicated the expected neutrino background to future direct dark matter detection experiments from [70] as a black line; it will be difficult to impossible to measure χ_1^0 -nucleon cross section smaller than this background. Unfortunately we see that significant regions in the NUH-NMSSM parameter space – notably for $M_{\chi_1^0} \lesssim 10$ GeV or $M_{\chi_1^0} \gtrsim 60$ GeV – may lead to such small cross sections.

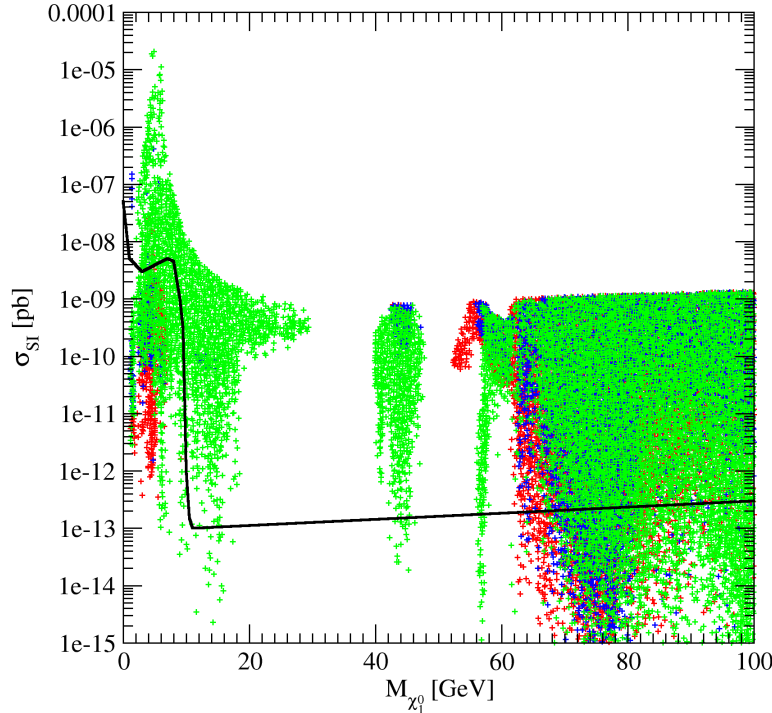


Figure 5: The spin-independent χ_1^0 -nucleon cross section σ_{SI} (after imposing constraints from the LUX experiment [5]) as function of $M_{\chi_1^0}$, focussing on $M_{\chi_1^0} < 100$ GeV. The black line indicates the expected neutrino background to future direct dark matter detection experiments (from [70]). The colors are as in Fig. 1.

Small χ_1^0 -nucleon cross sections originate from a large singlino component of χ_1^0 . Its singlino component N_{15}^2 is shown as function of $M_{\chi_1^0}$ in Fig. 6.

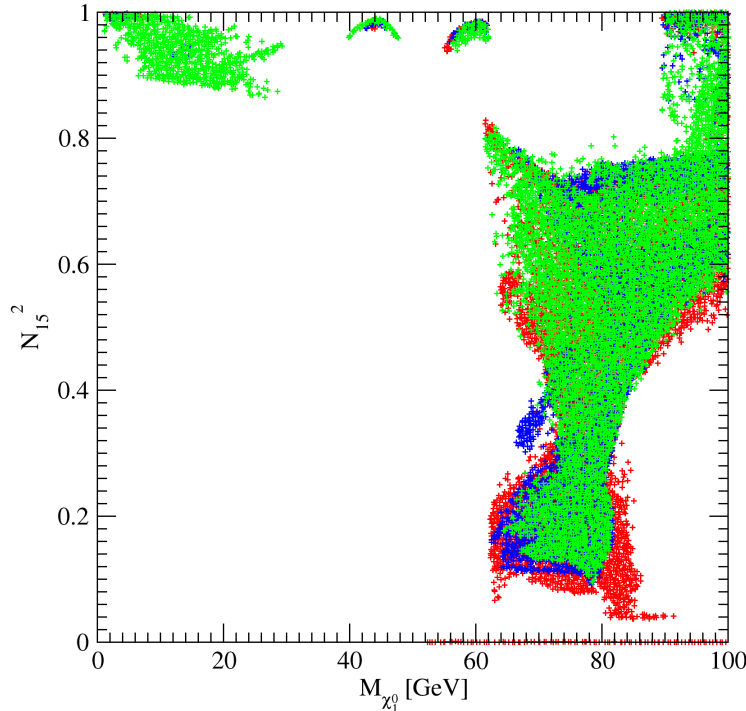


Figure 6: The χ_1^0 singlino component (squared) as function of $M_{\chi_1^0}$. The colors are as in Fig. 1.

Different regions of $M_{\chi_1^0}$ correspond to different dominant diagrams contributing to $\chi_1^0 - \chi_1^0$ annihilation before its freeze-out. For small $M_{\chi_1^0} \lesssim 30$ GeV these are the exchange of NMSSM-specific CP-even or CP-odd Higgs scalars with masses $\approx 2M_{\chi_1^0}$ in the s-channel, with couplings originating from the cubic S^3 term proportional to κ in the superpotential. For $M_{\chi_1^0} \sim 40 - 48$ GeV, $\chi_1^0 - \chi_1^0$ annihilation is dominated by Z -exchange in the s-channel. The larger is the singlino component of χ_1^0 , the closer $M_{\chi_1^0}$ has to be to $M_Z/2$ in order to compensate for the smaller coupling. For $M_{\chi_1^0} \sim 55 - 62$ GeV, $\chi_1^0 - \chi_1^0$ annihilation is dominated by H_{SM} -exchange. In the empty regions for $M_{\chi_1^0} \lesssim 55$ GeV, the non-singlet components of χ_1^0 would have to be so large for successful $\chi_1^0 - \chi_1^0$ annihilation that the χ_1^0 -nucleon cross section would violate constraints from LUX. For $M_{\chi_1^0} \gtrsim 62$ GeV χ_1^0 can have sizeable bino and/or higgsino components allowing for numerous additional (e.g. MSSM-like) $\chi_1^0 - \chi_1^0$ annihilation channels.

5 Properties of the lighter Higgs boson H_1

In this paper we focus on scenarios where mixing of the SM-like Higgs boson H_{SM} with a lighter NMSSM-specific mostly singlet-like Higgs boson H_1 helps to increase the mass of H_{SM} .

This is possible even for relatively small values of $\lambda \approx 0.1$ and moderate to large values of $\tan\beta$ [71].

However, the $H_{SM} - H_1$ mixing angle must not be too large: It leads to a reduction of the H_{SM} couplings to electroweak gauge bosons and quarks, hence to a reduction of its production cross section at the LHC. These must comply with the measured signal rates, for which we require values inside the 95% CL contours of [51]. Moreover, for $M_{H_1} \lesssim 114$ GeV, H_1 must satisfy constraints from Higgs searches at LEP [72].

Hence the question is whether there are realistic prospects for the discovery of H_1 at the LHC [73]. First we consider the case where H_1 does not decay dominantly into pairs of lighter NMSSM-specific CP-odd Higgs bosons. The branching fractions of H_1 into ZZ and W^+W^- are small, both due to its smaller mass and its reduced couplings to ZZ and W^+W^- .

The branching fraction of H_1 into $\gamma\gamma$ can be considerably larger than the one of a SM-like Higgs boson of the same mass [71, 74], both due to a possible reduction of its width into the dominant $b\bar{b}$ channel through mixing, and/or due to additional (higgsino-like) chargino loops contributing to the $H_1 - \gamma\gamma$ coupling where the latter involve the NMSSM-specific coupling λ [75, 76].

However, due to the reduced coupling of H_1 to SM particles, its production cross section σ_{H_1} is smaller than the one of a SM Higgs boson H^{SM} of the same mass. Hence one has to consider the reduced signal rate $\sigma_{H_1} \times BR(H_1 \rightarrow \gamma\gamma) / (\sigma_{H^{SM}} \times BR(H^{SM} \rightarrow \gamma\gamma))$ [71, 74, 77, 78] which is shown for production via gluon fusion in Fig. 7.

We see that the signal rate can be about 3.5 times larger than the one of a SM-like Higgs boson of a mass of ~ 60 GeV. The absence of points with large signal rates for $M_{H_1} \lesssim 60$ GeV follows from the constraints on the signal rates of H_{SM} : For $M_{H_1} \lesssim 60$ GeV, H_{SM} could decay into a pair of H_1 bosons, and this decay channel is easily dominant if kinematically allowed. The corresponding reductions of the other H_{SM} branching fractions would be incompatible with its measured signal rates. (The possible enhancement of the signal rate for $M_{H_1} \lesssim 3.5$ GeV originates from the absence of decays into $b\bar{b}$ and $\tau^+\tau^-$, which makes it very sensitive to relative enhancements of the width into $\gamma\gamma$ via chargino loops.) For $M_{H_1} \gtrsim 110$ GeV, some points with a reduced signal rate $\gtrsim 0.5$ could actually already be excluded by limits from CMS in [79] depending, however, on the relative contribution of gluon fusion to the expected signal rate in this mass range. On the other hand it is clear that, for $M_{H_1} \sim M_Z$, the $H_1 \rightarrow \gamma\gamma$ channel faces potentially large backgrounds from fake photons from $Z \rightarrow e^+e^-$ decays.

For the $b\bar{b}$ and $\tau^+\tau^-$ final states we found that due to the reduction of the production cross section and the reduction of the couplings (i.e. branching fractions) of H_1 its reduced signal rates in gluon fusion, vector boson fusion and associate production with Z/W are always below 0.3 for $M_{H_1} \lesssim 114$ GeV, and still below 0.6 for $114 \text{ GeV} \lesssim M_{H_1} \lesssim 126$ GeV; hence we will not further analyse these channels (also plagued by the absence of narrow peaks in the invariant mass of the final states).

Another possibility is that H_1 decays dominantly into pairs of light NMSSM-specific CP-odd Higgs bosons A_1 (see [80] and refs. therein). If this channel is open, the corresponding branching fraction $BR(H_1 \rightarrow A_1 A_1)$ can vary from 0 to 1 for all M_{H_1} and M_{A_1} . However, the production cross section of H_1 is always reduced relative to the one of a SM-like Higgs boson H^{SM} of the same mass. Focussing again on gluon fusion, we show in Figs. 8 the $BR(H_1 \rightarrow A_1 A_1)$ multiplied by the reduced H_1 production cross section (relative to the one of a SM-like Higgs

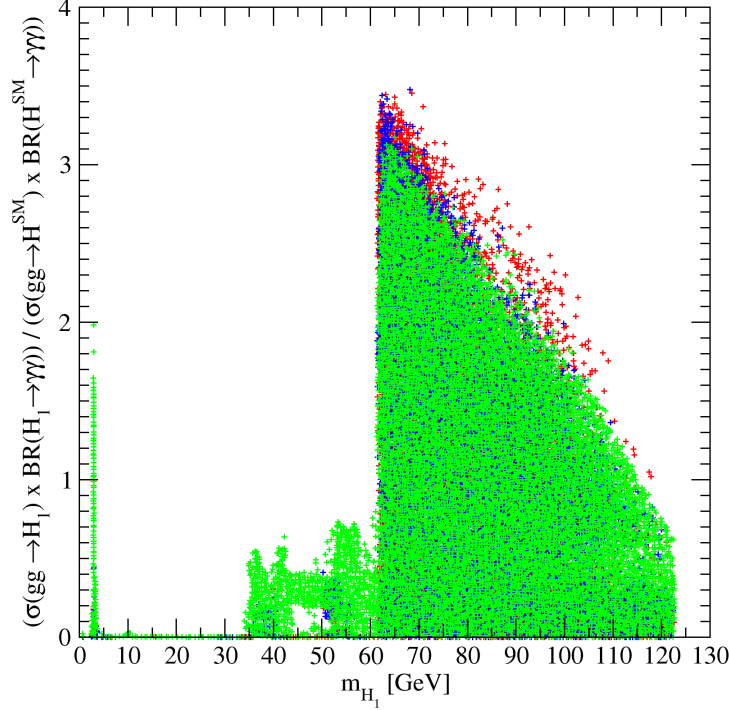


Figure 7: The H_1 signal rate in gluon fusion and the $\gamma\gamma$ channel relative to a SM-like Higgs boson H^{SM} of the same mass. The color code is as in Fig. 1.

boson H^{SM} of the same mass) as function of M_{H_1} and M_{A_1} .

The dominant decay branching fractions of A_1 are very similar to the ones of a SM-like Higgs boson of the same mass, i.e. dominantly into $b\bar{b}$ and $\tau^+\tau^-$ if kinematically allowed. These unconventional channels $H \rightarrow A_1 A_1 \rightarrow \dots$ have been searched for at LEP by OPAL [81–83], DELPHI [84] and ALEPH [85]. The corresponding constraints are taken into account in NMSSMTools, and explain the absence of sizeable signal rates for $M_{H_1} \lesssim 80$ GeV. For $M_{H_1} \gtrsim 86$ GeV and, simultaneously, 0.25 GeV $\lesssim M_{A_1} \lesssim 3.55$ GeV, first LHC analyses by CMS [86] have lead to upper limits on the signal cross section for $H \rightarrow A_1 A_1 \rightarrow 4\mu$ which exclude some of the points in this range of M_{A_1} .

For heavier A_1 leading to dominant $b\bar{b}$ and/or $\tau^+\tau^-$ decays, analyses of possible signals are certainly more difficult. At least we find that, for $M_{H_1} \gtrsim 80$ GeV, production cross sections times branching fractions can be relatively large without violating present constraints, which should motivate future analyses of these channels.

Concerning the signal rates of the SM-like Higgs boson H_2 we remark that all values allowed by the 95% confidence level contours in [51] in the planes of Higgs production via (gluon fusion and $t\bar{t}H$) – (vector boson fusion and associate production with W/Z) for Higgs decays into $\gamma\gamma$, $ZZ+WW$ and $b\bar{b} + \tau^+\tau^-$ have been found by our scan.

Also possible are decays of H_2 into pairs of light CP-even or CP-odd states H_1 or A_1 . They

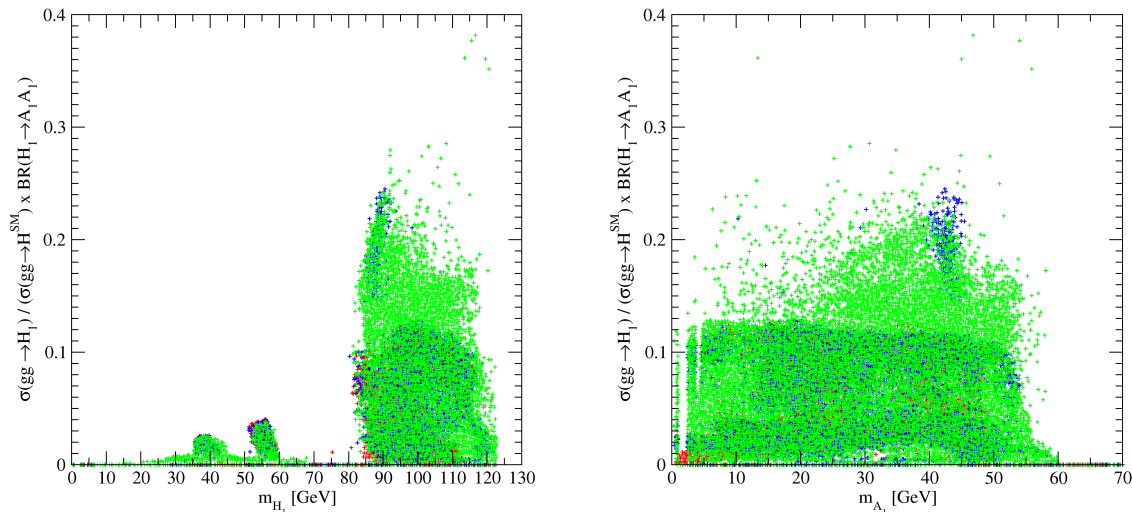


Figure 8: $\sigma_{H_1}(ggF)/\sigma_{H^{SM}}(ggF) \times BR(H_1 \rightarrow A_1 A_1)$ as function of M_{H_1} (left) and M_{A_1} (right). The color coding is as in Fig. 1.

are limited by the SM-like signal rates of H_2 , but branching fractions of up to 40% are still allowed.

6 Conclusions and outlook

In spite of the recent constraints on the mass and the signal rates at the LHC on a SM-like Higgs boson, upper bounds on signal rates generated by first generation squarks and gluinos and upper bounds on dark matter – nucleus cross sections we have seen that large ranges of the parameter space of the NUH-NMSSM remain viable. Within this scenario, bounds from squark/gluino searches dominate the lower bounds on fine-tuning which remain, on the other hand, considerably smaller than in the (NUHM-)MSSM and more constrained versions of the NMSSM.

The mass of the LSP is barely constrained, up to some “holes” around 30 and 50 GeV, and can possibly be below 1 GeV. Due to its possibly dominant singlino component, its direct detection cross section can be considerably smaller than the neutrino background, which makes it compatible with all future null-results in direct (and actually also indirect) dark matter searches.

We have not discussed all possible NUH-NMSSM-specific phenomena at colliders, which would be beyond the scope of the present paper. Here we focussed on the properties of an additional lighter NMSSM-specific Higgs boson H_1 , in particular on its signal rates in channels which are accessible at the LHC. These include the potentially promising diphoton decay channel, but also H_1 -decays into a pair of even lighter CP-odd bosons A_1 . Albeit taking into account all present constraints on additional lighter Higgs bosons, wide ranges of H_1 and A_1 masses remain to be explored.

Amongst additional NUH-NMSSM-specific phenomena at colliders – induced by a sing-

lino-like LSP and/or additional Higgs states – are possibly unconventional cascade decays of charginos and top- and bottom-squarks, which require additional studies. Future work will also be dedicated to the possibilities for and signatures of Higgs-to-Higgs decay cascades induced by heavier Higgs states in the NUH-NMSSM.

Acknowledgements

UE acknowledges support from the ERC advanced grant Higgs@LHC and from the European Union Initial Training Networks INVISIBLES (PITN-GA-2011-289442) and HiggsTools (PITN-GA-2012-316704). The authors acknowledge the support of France Grilles for providing computing resources on the French National Grid Infrastructure.

References

- [1] G. Aad *et al.* [ATLAS Collaboration], Phys. Lett. B **716** (2012) 1 [arXiv:1207.7214 [hep-ex]].
- [2] S. Chatrchyan *et al.* [CMS Collaboration], Phys. Lett. B **716** (2012) 30 [arXiv:1207.7235 [hep-ex]].
- [3] The ATLAS collaboration, “Search for squarks and gluinos with the ATLAS detector in final states with jets and missing transverse momentum and 20.3 fb⁻¹ of $\sqrt{s} = 8$ TeV proton-proton collision data,” ATLAS-CONF-2013-047.
- [4] S. Chatrchyan *et al.* [CMS Collaboration], “Search for new physics in the multijet and missing transverse momentum final state in proton-proton collisions at $\sqrt{s} = 8$ TeV,” arXiv:1402.4770 [hep-ex].
- [5] D. S. Akerib *et al.* [LUX Collaboration], Phys. Rev. Lett. **112**, 091303 (2014) [arXiv:1310.8214 [astro-ph.CO]].
- [6] H. Baer, V. Barger and A. Mustafayev, Phys. Rev. D **85** (2012) 075010 [arXiv:1112.3017 [hep-ph]].
- [7] A. Arbey, M. Battaglia, A. Djouadi, F. Mahmoudi and J. Quevillon, Phys. Lett. B **708** (2012) 162 [arXiv:1112.3028 [hep-ph]].
- [8] O. Buchmueller, R. Cavanaugh, A. De Roeck, M. J. Dolan, J. R. Ellis, H. Flacher, S. Heinemeyer and G. Isidori *et al.*, Eur. Phys. J. C **72** (2012) 2020 [arXiv:1112.3564 [hep-ph]].
- [9] S. Akula, B. Altunkaynak, D. Feldman, P. Nath and G. Peim, Phys. Rev. D **85** (2012) 075001 [arXiv:1112.3645 [hep-ph]].
- [10] M. Kadastik, K. Kannike, A. Racioppi and M. Raidal, JHEP **1205** (2012) 061 [arXiv:1112.3647 [hep-ph]].
- [11] J. Cao, Z. Heng, D. Li and J. M. Yang, Phys. Lett. B **710** (2012) 665 [arXiv:1112.4391 [hep-ph]].
- [12] J. Ellis and K. A. Olive, Eur. Phys. J. C **72** (2012) 2005 [arXiv:1202.3262 [hep-ph]].
- [13] A. Fowlie, M. Kazana, K. Kowalska, S. Munir, L. Roszkowski, E. M. Sessolo, S. Trojanowski and Y. -L. S. Tsai, Phys. Rev. D **86** (2012) 075010 [arXiv:1206.0264 [hep-ph]].
- [14] C. Beskidt, W. de Boer, D. I. Kazakov and F. Ratnikov, Eur. Phys. J. C **72** (2012) 2166 [arXiv:1207.3185 [hep-ph]].
- [15] O. Buchmueller, R. Cavanaugh, M. Citron, A. De Roeck, M. J. Dolan, J. R. Ellis, H. Flacher and S. Heinemeyer *et al.*, Eur. Phys. J. C **72** (2012) 2243 [arXiv:1207.7315].
- [16] C. Strege, G. Bertone, F. Feroz, M. Fornasa, R. Ruiz de Austri and R. Trotta, [arXiv:1212.2636 [hep-ph]].

- [17] J. Ellis, F. Luo, K. A. Olive and P. Sandick, Eur. Phys. J. C **73** (2013) 2403 [arXiv:1212.4476 [hep-ph]].
- [18] M. E. Cabrera, J. A. Casas and R. R. de Austri, JHEP **1307** (2013) 182 [arXiv:1212.4821 [hep-ph]].
- [19] K. Kowalska, L. Roszkowski and E. M. Sessolo, JHEP **1306** (2013) 078 [arXiv:1302.5956 [hep-ph]].
- [20] T. Cohen and J. G. Wacker, JHEP **1309** (2013) 061 [arXiv:1305.2914 [hep-ph]].
- [21] C. Beskidt, W. de Boer and D. I. Kazakov, Phys. Lett. B **726** (2013) 758 [arXiv:1308.1333 [hep-ph]].
- [22] S. Henrot-Versillé, R. Lafaye, T. Plehn, M. Rauch, D. Zerwas, S. Plaszczynski, B. Rouillé d’Orfeuil and M. Spinelli, Phys. Rev. D **89** (2014) 055017 [arXiv:1309.6958 [hep-ph]].
- [23] P. Bechtle, K. Desch, H. K. Dreiner, M. Hamer, M. Krämer, B. O’Leary, W. Porod and X. Prudent *et al.*, “Constrained Supersymmetry after the Higgs Boson Discovery: A global analysis with Fittino,” arXiv:1310.3045 [hep-ph].
- [24] D. Kim, P. Athron, C. Balázs, B. Farmer and E. Hutchison, “Bayesian naturalness of the C(N)MSSM,” arXiv:1312.4150 [hep-ph].
- [25] O. Buchmueller, R. Cavanaugh, A. De Roeck, M. J. Dolan, J. R. Ellis, H. Flacher, S. Heinemeyer and G. Isidori *et al.*, “The CMSSM and NUHM1 after LHC Run 1,” arXiv:1312.5250 [hep-ph].
- [26] J. Ellis, “Supersymmetric Fits after the Higgs Discovery and Implications for Model Building,” arXiv:1312.5426 [hep-ph].
- [27] J. F. Gunion, Y. Jiang and S. Kraml, Phys. Lett. B **710** (2012) 454 [arXiv:1201.0982 [hep-ph]].
- [28] U. Ellwanger and C. Hugonie, Adv. High Energy Phys. **2012** (2012) 625389 [arXiv:1203.5048 [hep-ph]].
- [29] G. Belanger, U. Ellwanger, J. F. Gunion, Y. Jiang, S. Kraml and J. H. Schwarz, JHEP **1301** (2013) 069 [arXiv:1210.1976 [hep-ph]].
- [30] K. Kowalska *et al.* [BayesFITS Group Collaboration], Phys. Rev. D **87** (2013) 11, 115010 [arXiv:1211.1693 [hep-ph]].
- [31] C. Beskidt, W. de Boer and D. I. Kazakov, “The impact of a 126 GeV Higgs on the neutralino mass,” arXiv:1402.4650 [hep-ph].
- [32] Z. Kang, J. Li and T. Li, JHEP **1211** (2012) 024 [arXiv:1201.5305 [hep-ph]].
- [33] J. -J. Cao, Z. -X. Heng, J. M. Yang, Y. -M. Zhang and J. -Y. Zhu, JHEP **1203** (2012) 086 [arXiv:1202.5821 [hep-ph]].

- [34] D. A. Vasquez, G. Belanger, C. Boehm, J. Da Silva, P. Richardson and C. Wymant, Phys. Rev. D **86** (2012) 035023 [arXiv:1203.3446 [hep-ph]].
- [35] M. Perelstein and B. Shakya, Phys. Rev. D **88** (2013) 075003 [arXiv:1208.0833 [hep-ph]].
- [36] K. Agashe, Y. Cui and R. Franceschini, JHEP **1302** (2013) 031 [arXiv:1209.2115 [hep-ph]].
- [37] T. Gherghetta, B. von Harling, A. D. Medina and M. A. Schmidt, JHEP **02** (2013) 032 [arXiv:1212.5243 [hep-ph]].
- [38] T. Cheng, J. Li, T. Li and Q. -S. Yan, Phys. Rev. D **89** (2014) 015015 [arXiv:1304.3182 [hep-ph]].
- [39] J. Cao, F. Ding, C. Han, J. M. Yang and J. Zhu, JHEP **1311** (2013) 018 [arXiv:1309.4939 [hep-ph]].
- [40] U. Ellwanger and C. Hugonie, Comput. Phys. Commun. **177** (2007) 399 [hep-ph/0612134].
- [41] U. Ellwanger, J. F. Gunion and C. Hugonie, JHEP **0502** (2005) 066 [hep-ph/0406215].
- [42] U. Ellwanger and C. Hugonie, Comput. Phys. Commun. **175** (2006) 290 [hep-ph/0508022].
- [43] G. Belanger, F. Boudjema, A. Pukhov and A. Semenov, Comput. Phys. Commun. **185** (2014) 960 [arXiv:1305.0237 [hep-ph]].
- [44] U. Ellwanger, C. Hugonie and A. M. Teixeira, Phys. Rept. **496** (2010) 1 [arXiv:0910.1785 [hep-ph]].
- [45] L. J. Hall, D. Pinner and J. T. Ruderman, JHEP **1204** (2012) 131 [arXiv:1112.2703 [hep-ph]].
- [46] U. Ellwanger, JHEP **1203** (2012) 044 [arXiv:1112.3548 [hep-ph]].
- [47] A. Arvanitaki and G. Villadoro, JHEP **1202** (2012) 144 [arXiv:1112.4835 [hep-ph]].
- [48] S. F. King, M. Muhlleitner and R. Nevzorov, Nucl. Phys. B **860** (2012) 207 [arXiv:1201.2671 [hep-ph]].
- [49] G. Hinshaw *et al.* [WMAP Collaboration], Astrophys. J. Suppl. **208** (2013) 19 [arXiv:1212.5226 [astro-ph.CO]].
- [50] P. A. R. Ade *et al.* [Planck Collaboration], “Planck 2013 results. XVI. Cosmological parameters,” arXiv:1303.5076 [astro-ph.CO].
- [51] G. Belanger, B. Dumont, U. Ellwanger, J. F. Gunion and S. Kraml, Phys. Rev. D **88** (2013) 075008 [arXiv:1306.2941 [hep-ph]].
- [52] D. Das, U. Ellwanger and A. M. Teixeira, JHEP **1204** (2012) 067 [arXiv:1202.5244 [hep-ph]].

- [53] D. Das, U. Ellwanger and A. M. Teixeira, JHEP **1304** (2013) 117 [arXiv:1301.7584 [hep-ph]].
- [54] J. Alwall, M. Herquet, F. Maltoni, O. Mattelaer and T. Stelzer, JHEP **1106** (2011) 128 [arXiv:1106.0522 [hep-ph]].
- [55] T. Sjostrand, S. Mrenna and P. Z. Skands, JHEP **0605** (2006) 026 [hep-ph/0603175].
- [56] D. Das, U. Ellwanger and A. M. Teixeira, Comput. Phys. Commun. **183** (2012) 774 [arXiv:1106.5633 [hep-ph]].
- [57] M. Muhlleitner, A. Djouadi and Y. Mambrini, Comput. Phys. Commun. **168** (2005) 46 [arXiv:hep-ph/0311167].
- [58] M. Drees, H. Dreiner, D. Schmeier, J. Tattersall and J. S. Kim, “CheckMATE: Confronting your Favourite New Physics Model with LHC Data,” arXiv:1312.2591 [hep-ph].
- [59] J. de Favereau *et al.* [DELPHES 3 Collaboration], JHEP **1402** (2014) 057 [arXiv:1307.6346 [hep-ex]].
- [60] R. Barbieri and G. F. Giudice, Nucl. Phys. B **306** (1988) 63.
- [61] U. Ellwanger, G. Espitalier-Noel and C. Hugonie, JHEP **1109** (2011) 105 [arXiv:1107.2472 [hep-ph]].
- [62] A. Djouadi, U. Ellwanger and A. M. Teixeira, Phys. Rev. Lett. **101** (2008) 101802 [arXiv:0803.0253 [hep-ph]].
- [63] A. Djouadi, U. Ellwanger and A. M. Teixeira, JHEP **0904** (2009) 031 [arXiv:0811.2699 [hep-ph]].
- [64] H. Baer, V. Barger, P. Huang, D. Mickelson, A. Mustafayev and X. Tata, Phys. Rev. D **87** (2013) 11, 115028 [arXiv:1212.2655 [hep-ph]].
- [65] M. Y. Binjonaïd and S. F. King, “Naturalness of scale-invariant NMSSMs with and without extra matter,” arXiv:1403.2088 [hep-ph].
- [66] U. Ellwanger and C. Hugonie, Eur. Phys. J. C **25** (2002) 297 [arXiv:hep-ph/9909260].
- [67] G. Belanger, F. Boudjema, C. Hugonie, A. Pukhov and A. Semenov, JCAP **0509** (2005) 001 [hep-ph/0505142].
- [68] C. Hugonie, G. Belanger and A. Pukhov, JCAP **0711** (2007) 009 [arXiv:0707.0628 [hep-ph]].
- [69] G. Belanger, C. Hugonie and A. Pukhov, JCAP **0901** (2009) 023 [arXiv:0811.3224 [hep-ph]].
- [70] J. Billard, L. Strigari and E. Figueroa-Feliciano, Phys. Rev. D **89** (2014) 023524 [arXiv:1307.5458 [hep-ph]].

- [71] M. Badziak, M. Olechowski and S. Pokorski, JHEP **1306** (2013) 043 [arXiv:1304.5437 [hep-ph]].
- [72] S. Schael *et al.* [ALEPH and DELPHI and L3 and OPAL Collaborations and LEP Working Group for Higgs Boson Searches], Eur. Phys. J. C **47** (2006) 547 [arXiv:hep-ex/0602042].
- [73] G. Cacciapaglia, A. Deandrea, G. D. La Rochelle and J. -B. Flament, “Searching for a lighter Higgs: parametrisation and sample tests,” arXiv:1311.5132 [hep-ph].
- [74] U. Ellwanger, Phys. Lett. B **698** (2011) 293 [arXiv:1012.1201 [hep-ph]].
- [75] K. Schmidt-Hoberg and F. Staub, JHEP **1210** (2012) 195 [arXiv:1208.1683 [hep-ph]].
- [76] K. Choi, S. H. Im, K. S. Jeong and M. Yamaguchi, JHEP **1302** (2013) 090 [arXiv:1211.0875 [hep-ph]].
- [77] J. Cao, Z. Heng, T. Liu and J. M. Yang, Phys. Lett. B **703** (2011) 462 [arXiv:1103.0631 [hep-ph]].
- [78] S. F. King, M. Mühlleitner, R. Nevzorov and K. Walz, Nucl. Phys. B **870** (2013) 323 [arXiv:1211.5074 [hep-ph]].
- [79] CMS Collaboration, “Updated measurements of the Higgs boson at 125 GeV in the two photon decay channel,” CMS-PAS-HIG-13-001
- [80] D. G. Cerdeno, P. Ghosh and C. B. Park, JHEP **1306** (2013) 031 [arXiv:1301.1325 [hep-ph]].
- [81] G. Abbiendi *et al.* [OPAL Collaboration], Eur. Phys. J. C **27** (2003) 311 [arXiv:hep-ex/0206022].
- [82] G. Abbiendi *et al.* [OPAL Collaboration], Eur. Phys. J. C **37** (2004) 49 [arXiv:hep-ex/0406057].
- [83] G. Abbiendi *et al.* [OPAL Collaboration], Eur. Phys. J. C **27** (2003) 483 [arXiv:hep-ex/0209068].
- [84] J. Abdallah *et al.* [DELPHI Collaboration], Eur. Phys. J. C **38** (2004) 1 [arXiv:hep-ex/0410017].
- [85] S. Schael *et al.* [ALEPH Collaboration], JHEP **1005** (2010) 049 [arXiv:1003.0705].
- [86] S. Chatrchyan *et al.* [CMS Collaboration], Phys. Lett. B **726** (2013) 564 [arXiv:1210.7619 [hep-ex]].